Figures

Figure 1: Location of the ice camp located near the Qikiqtarjuaq Island in the Baffin Bay. Projection used: EPSG-4326.

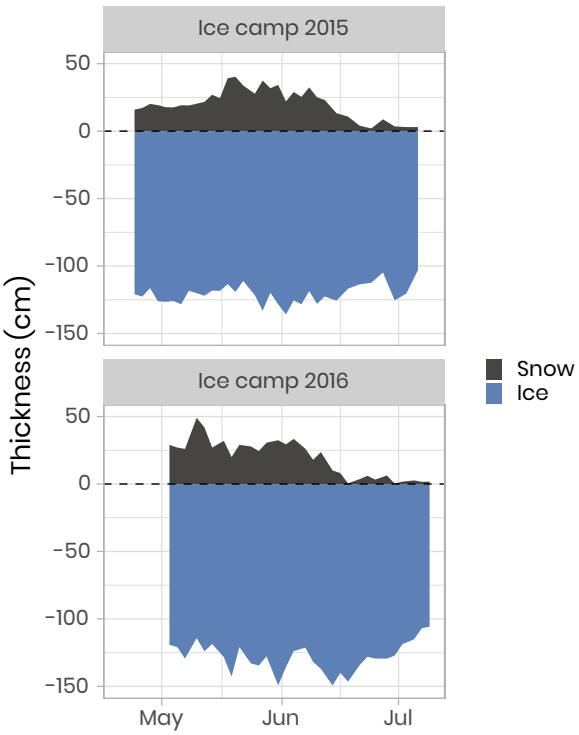

Figure 2: Temporal evolution of the snow and sea-ice thickness for both ice camp missions. The dashed horizontal line represents the snow/ice interface.

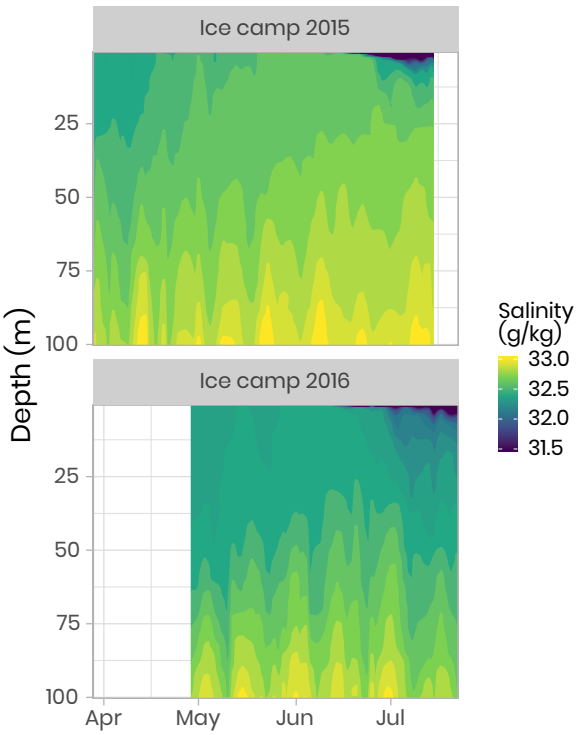

Figure 3: Temporal evolution of the salinity in the first 100 meters of the water column for both campaigns. Note that for visualization, salinity below 31.5 g kg^{-1} have been binned to 31.5 g kg^{-1}.

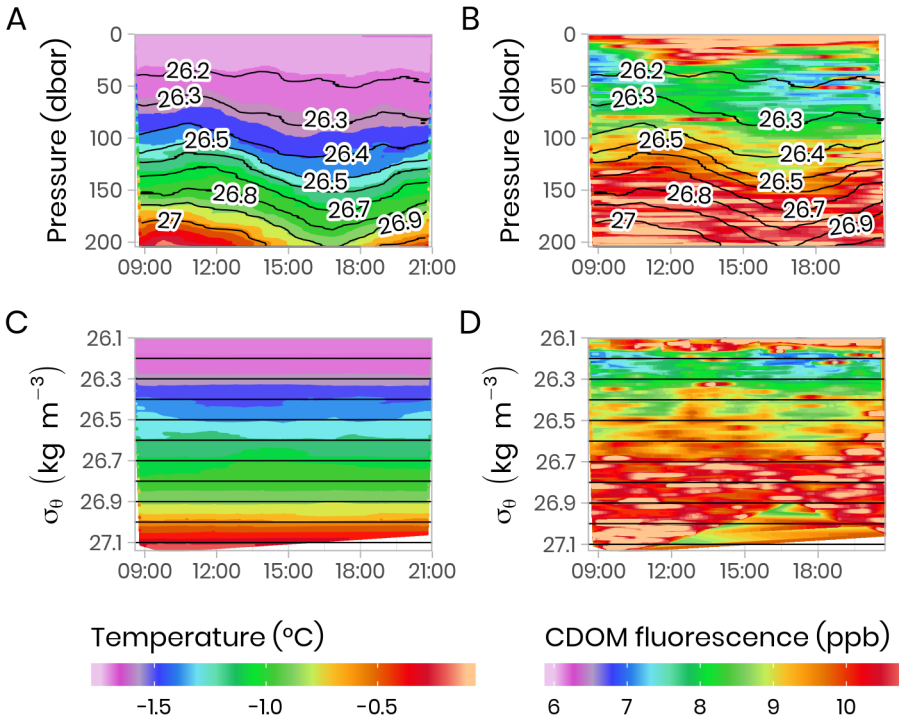

Figure 4: Temporal evolution of physical (temperature) and bio-optical (CDOM fluorescence) variables with superimposed lines of potential density anomaly (σ_θ, kg m^{-3}) during a 13-h tidal cycle. Surface tidal height versus time at Qikiqtarjuaq is shown in blue. (**A-B**) Plotted versus pressure coordinates (equivalent to depth in meters). (**C-D**) The same data plotted versus potential density anomaly σ_θ coordinates (kg m^{-3}). The tidal survey was performed on 2015-06-09.

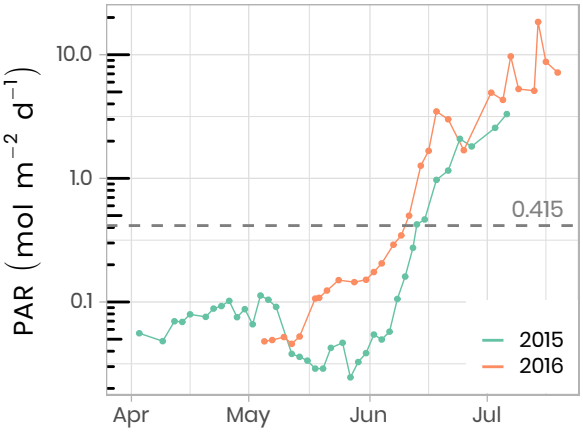

Figure 5: Temporal evolution of daily photosynthetically available radiation (PAR) at the sea-ice/water interface (1.3 m depth) for both ice camp missions. The horizontal dashed line shows the 0.415 mol photons m^{-2} d^{-1} threshold often used in the literature as the minimum light requirement for primary production.

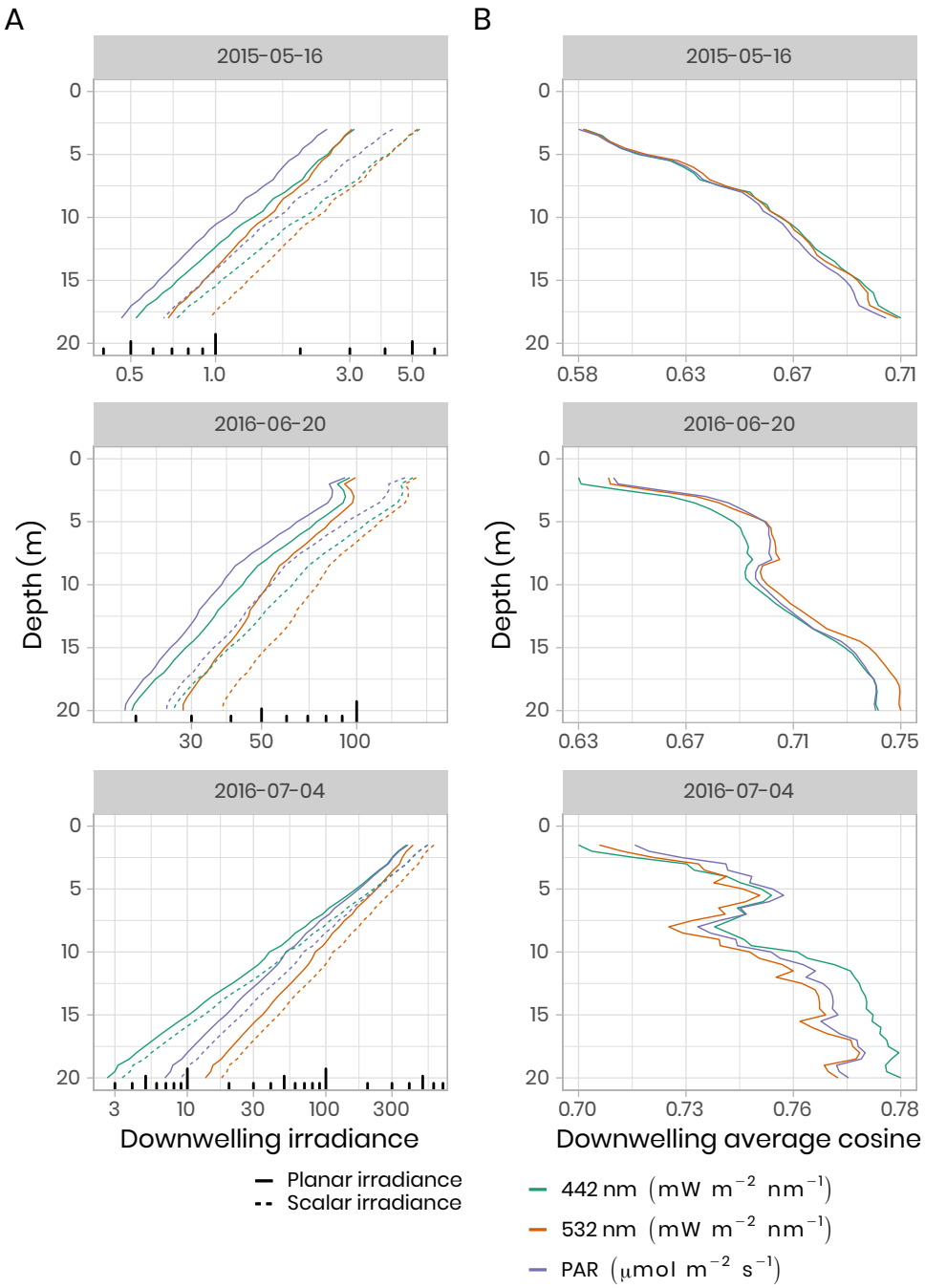

Figure 6: (**A**) Under-ice vertical profiles of downwelling planar and scalar irradiance at 442 nm, 532 nm and for PAR. Note the log scale for the irradiance measurements. (**B**) Calculated downwelling average cosine (unitless) was measured beneath snow-covered sea ice on 16 May 2015, beneath bare ice on 20 June 2016 and beneath a melt pond on 4 July 2016.

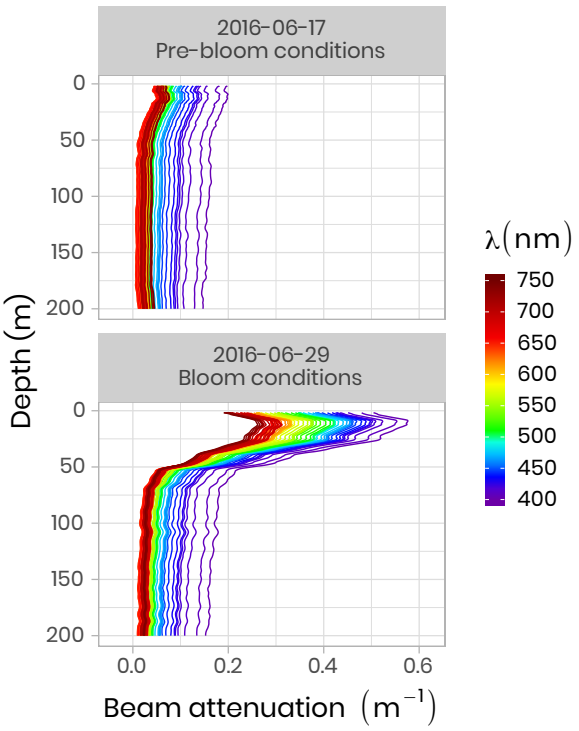

Figure 7: Beam attenuation coefficients (c, m^{-1}) measured in 2016 using an ACS before and during the phytoplankton bloom. Note that the colors of the lines correspond to wavelength frequencies.

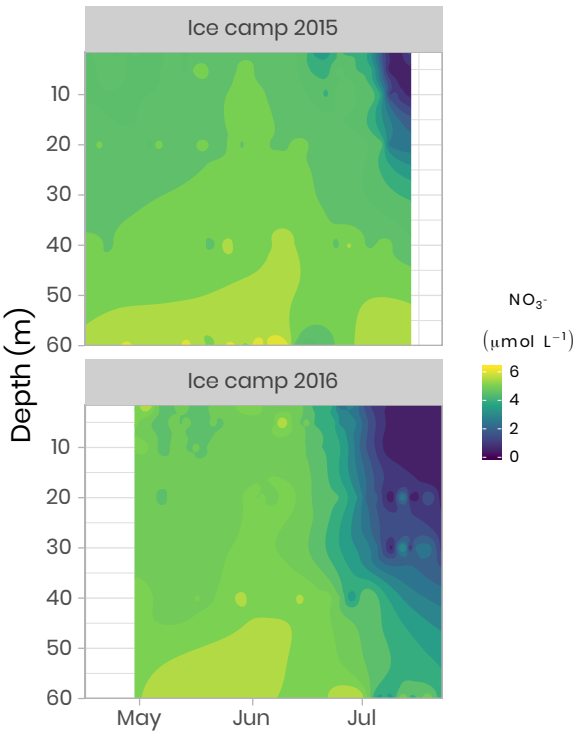

Figure 8: Temporal evolution of the nitrates in the first 60 m of the water column for both ice camp missions.

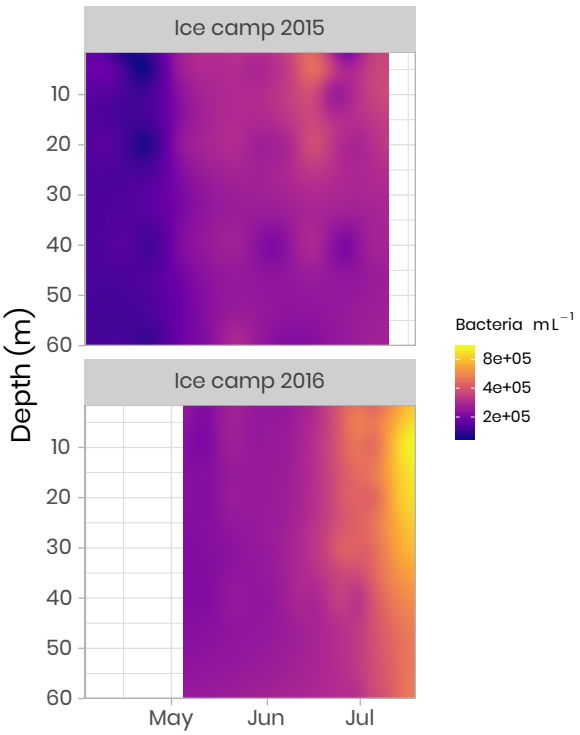

Figure 9: Concentration of bacteria in the water column at the ice camp in 2015 and 2016.

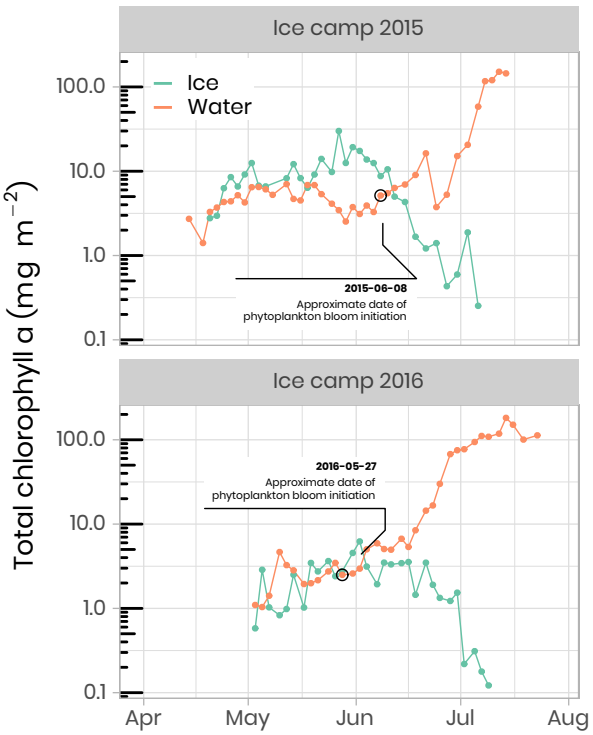

Figure 10: Temporal evolution of chlorophyll a in ice and water (depth-integrated) for both ice camp missions. Note that the water chlorophyll a have been integrated over the first 100 m of the water column whereas the ice chlorophyll a was measured on the bottom 0-10 cm of the ice cores. The details of the calculations to determine the approximate dates of phytoplankton bloom initiation can be found in Oziel et al. (2019).

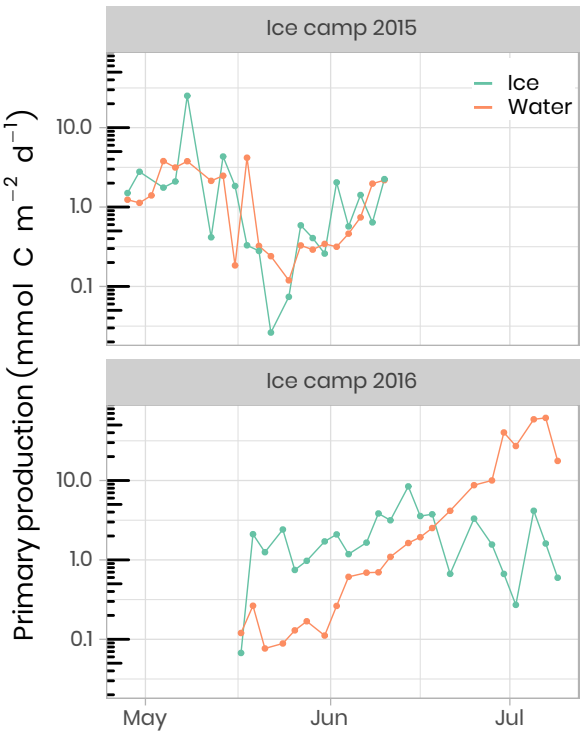

Figure 11: Temporal evolution of primary production a in ice and water (depth-integrated) for both ice camp missions.

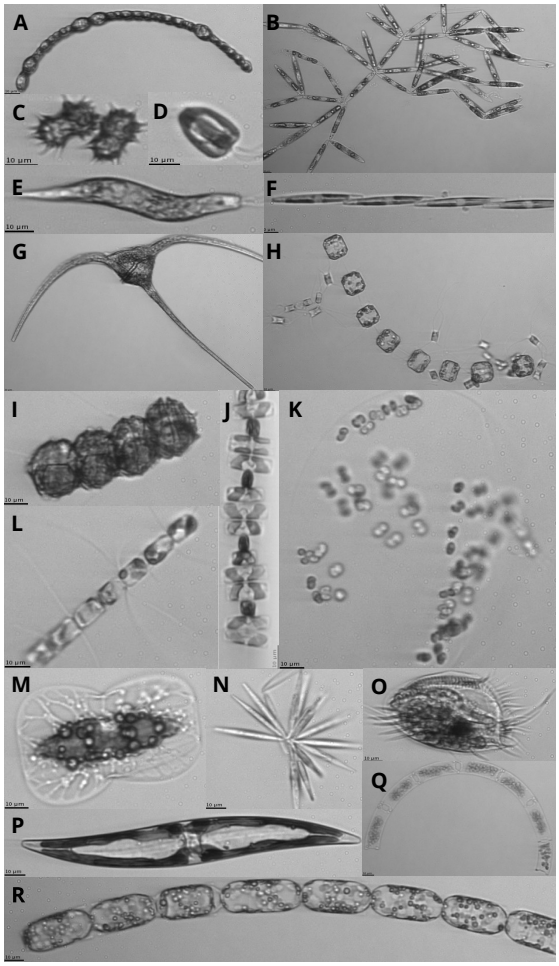

Figure 12: Images of protists sampled with the IFCB. Scale bar on images is 10 µm. Note that images are not to scale. (**A**) *Anabaena* sp. (**B**) *Nitzschia frigida* (**C**) *Polarella glacialis* (**D**) Flagellate (**E**) Euglena (**F**) *Pseudo-nitzschia* sp. (**G**) *Ceratium* sp. (**H**) *Thalassiosira nordenskioeldii* with *Attheya septentrionalis* (**I**) *Peridiniella catenata* (**J**) *Navicula pelagica* (**K**) *Phaeocystis* sp. colony (**L**) *Chaetoceros* sp. (**M**) *Entomoneis* sp. (**N**) *Synedropsis hyperborea* (**O**) Ciliate (**P**) Pennate diatom (**Q**) *Eucampia* sp. (**R**) *Melosira* sp.

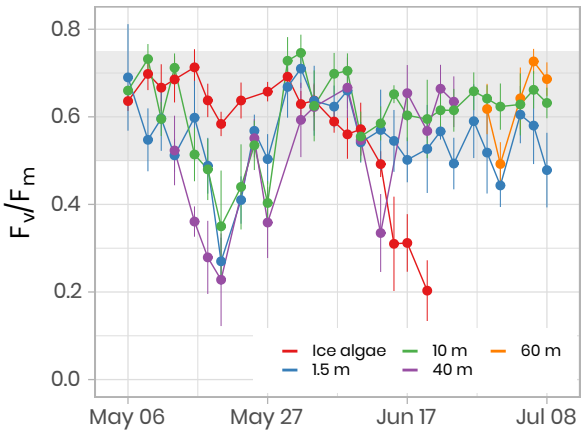

Figure 13: Temporal evolution of F_v/F_m for ice (last cm) and water underneath the ice (depths 1.5 m, 10 m, 40 m) samples for the ice camp 2016 between May 6th and July 8th. F_v/F_m monitoring on ice samples stopped on June 20th because the Chl a fluorescence signal was not reliable anymore. F_v/F_m monitoring on 40 m and 60 m depth samples was limited between May 13th and June 24th and between June 29th and July 08th, respectively. The gray shaded area represents the range at which the algae are optimally growing.

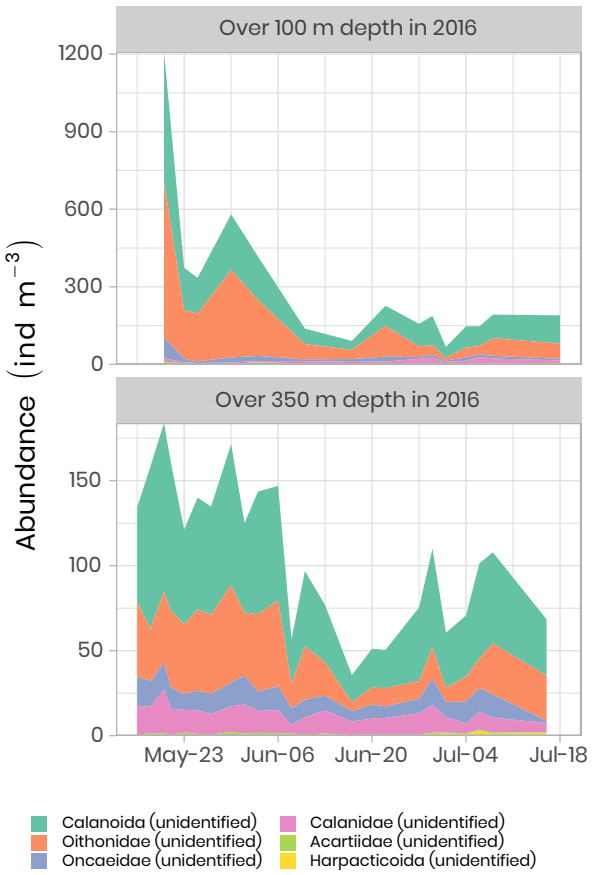

Figure 14: Time series of the abundance of the copepods (ind m^{-1}) measured over the first 100 m and 350 m of the water column in 2016 using the zooscan. For visualization, only the six most abundant groups are presented in decreasing order of importance. Note the different y-axes in both panels.